Title
Electrolytic Methane Production from Reactive Carbon Solutions

Journal
ACS Energy Letters, 7(5)

ISSN
2380-8195

Authors
Lees, Eric W
Liu, Alyssa
Bui, Justin C
et al.

Publication Date
2022-05-13

DOI
10.1021/acsenergylett.2c00283

Peer reviewed

Electrolytic methane production from reactive carbon solutions

Eric W. Lees,[1] Alyssa Liu,[2] Justin C. Bui,[3,4] Shaoxuan Ren,[2] Adam Z. Weber,[4*] and Curtis P. Berlinguette[1,2,5,6,*]

[1]Department of Chemical and Biological Engineering, The University of British Columbia, 2360 East Mall, Vancouver, British Columbia, V6T 1Z3, Canada.

[2]Department of Chemistry, The University of British Columbia, 2036 Main Mall, Vancouver, British Columbia, V6T 1Z1, Canada.

[3]Department of Chemical and Biomolecular Engineering, University of California, Berkeley, South Dr., Berkeley, CA 94720, USA

[4]Liquid Sunlight Alliance, Lawrence Berkeley National Laboratory, 1 Cyclotron Rd., Berkeley, CA 94720, USA

[5]Stewart Blusson Quantum Matter Institute, The University of British Columbia, 2355 East Mall, Vancouver, British Columbia, V6T 1Z4, Canada.

[6]Canadian Institute for Advanced Research (CIFAR), 661 University Avenue, Toronto, Ontario, M5G 1M1, Canada.

*Correspondence: cberling@chem.ubc.ca and azweber@lbl.gov

Abstract

We report here an electrochemical reactor that converts 3.0 M $KHCO_3$ into methane at the cathode, and oxidizes water at the anode. The molar ratio of methane product to unreacted CO_2 gas (defined herein as "methane yield") was measured to be *ca*. 30% at a partial current density of 120 mA cm^{-2}. The highest previously reported CO_2-to-methane yield is 3%. Our reactor achieved this improvement in methane yield because it is fed with 3.0 M $KHCO_3$, a type of reactive carbon solution, rather than gaseous CO_2. The reactor is designed so that H^+ delivered by the bipolar membrane reacts with HCO_3^- at the cathode to form CO_2. This CO_2 is then reduced to methane. A cationic surfactant added to the catholyte suppressed hydrogen evolution to increase the methane yield. A 1D continuum model confirmed that H^+ from the membrane promotes the formation of methane over multi-carbon products. These findings present design principles for electrochemical methane synthesis.

We report an electrochemical reactor that converts 3.0 M $KHCO_3$ into methane at the cathode, and oxidizes water at the anode. The molar ratio of methane product to unreacted CO_2 gas (defined herein as "methane yield") was measured to be 34% at a partial current density of 120 mA cm^{-2}. The highest previously reported CO_2-to-methane yield is 3%. Our reactor achieved this improvement in methane yield because it is fed with 3.0 M $KHCO_3$, a type of reactive carbon solution, rather than gaseous CO_2. The reactor uses H^+ delivered by a bipolar membrane to form CO_2 at the cathode. This CO_2 is subsequently reduced into methane. A cationic surfactant added to the catholyte suppressed hydrogen evolution and increased methane formation. A 1D continuum model confirmed that H^+ from the membrane promotes the formation of methane over multi-carbon products at the cathode. These findings present design principles for electrochemical methane synthesis.

The reduction of CO_2 into carbon-neutral chemicals and fuels could potentially store renewable energy and reduce greenhouse gas emissions. Methane is an appealing target because this fossil fuel stores more energy per mole of CO_2 (higher heating value: 802 kJ/mol CO_2) than any other CO_2-derived product and is used on a massive scale (~4 trillion cubic meters in 2019).[1,2] However, it is challenging to electrochemically convert CO_2 into methane;[3,4] the highest-performance electrochemical CO_2-to-CH_4 reactor yields a molar ratio of methane to CO_2 in the product stream ("methane yield") of only 3%. This methane yield needs to increase by at least an order-of-magnitude to be commercially relevant.[4]

All previously reported electrochemical systems that convert CO_2 to methane supply gaseous CO_2 to the cathode. Our program has instead focused on the electrochemical conversion of liquid (bi)carbonate solutions, a common eluent of carbon capture systems,[5] into higher-value carbon-containing products.[6,7] This electrochemical process would eliminate the expensive step of thermally extracting CO_2 and OH^- from (bi)carbonates.[5,8–10] (Reactive carbon solutions based on amines can also be electrochemically reduced to form CO_2 at the cathode.[11,12])

We have designed electrochemical reactors where protons supplied from the membrane (**Eq. 1**)[6,7,12] react with (bi)carbonate to form CO_2 at a porous cathode that is pressed against the membrane. The CO_2 that is generated *in situ* ("*i*-CO_2") is then reduced to carbon-containing products at the cathode. The liquid bicarbonate feedstock minimizes the amount of unreacted CO_2 in the product stream compared to a gaseous feedstock. Hence, the product yield for CO_2 reduction reaction (CO_2RR) products can be higher with liquid bicarbonate than with CO_2 gas.[13,14]

$$H^+_{(aq)} + HCO_3^-{}_{(aq)} \rightarrow CO_{2(g)} + H_2O_{(l)} \qquad \textbf{Eq. 1}$$

The other major consideration when designing such a reactor is the environment at the cathode. Copper is known to promote the formation of methane over multi-carbon products (e.g., ethylene) in

more acidic environments.[15,16] However, the pH is typically >12 at the cathode surface at high current densities (i > 200 mA cm^{-2}) because hydroxide is a CO2RR byproduct (**Eq. 2**).[17–19] This alkalinity suppresses the unwanted hydrogen evolution reaction (HER; **Eq. 3**),[20] but it also suppresses the protonation steps needed to form methane (**Eq. 2**).[16,21] These alkaline conditions instead promote the formation of multi-carbon products.[16,22]

$$CO_{2(aq)} + H_2O_{(l)} + 8e^- \rightarrow CH_{4(g)} + 8OH^-_{(aq)} \quad \textbf{Eq. 2}$$

$$2H^+_{(aq)} + 2e^- \rightarrow H_{2(g)} \quad \textbf{Eq. 3}$$

These observations prompted us to design and build an electrochemical reactor capable of converting potassium bicarbonate ($KHCO_3$) into methane. The membrane electrode assembly (MEA) of the reactor contains a bipolar membrane (BPM) that supplies protons to a porous copper cathode to convert $KHCO_3$ into i-CO_2 (**Eq. 1**), which is then reduced to methane (**Eq. 2**). A cationic surfactant was added to the electrolyte to suppress HER at the cathode (**Eq. 3**). This electrochemical reactor yielded a partial current density for methane formation (i_{CH4}) of 120 ± 10 mA cm^{-2} and methane yield of 34 ± 7%. This methane yield is 10-fold higher than any other documented reactor (**Fig. 1**). We developed a 1D continuum model to map out the dynamic reaction chemistry within the electrochemical reactor. This model shows that avoiding extreme alkalinity in the reactor can favor methane formation over multi-carbon products.

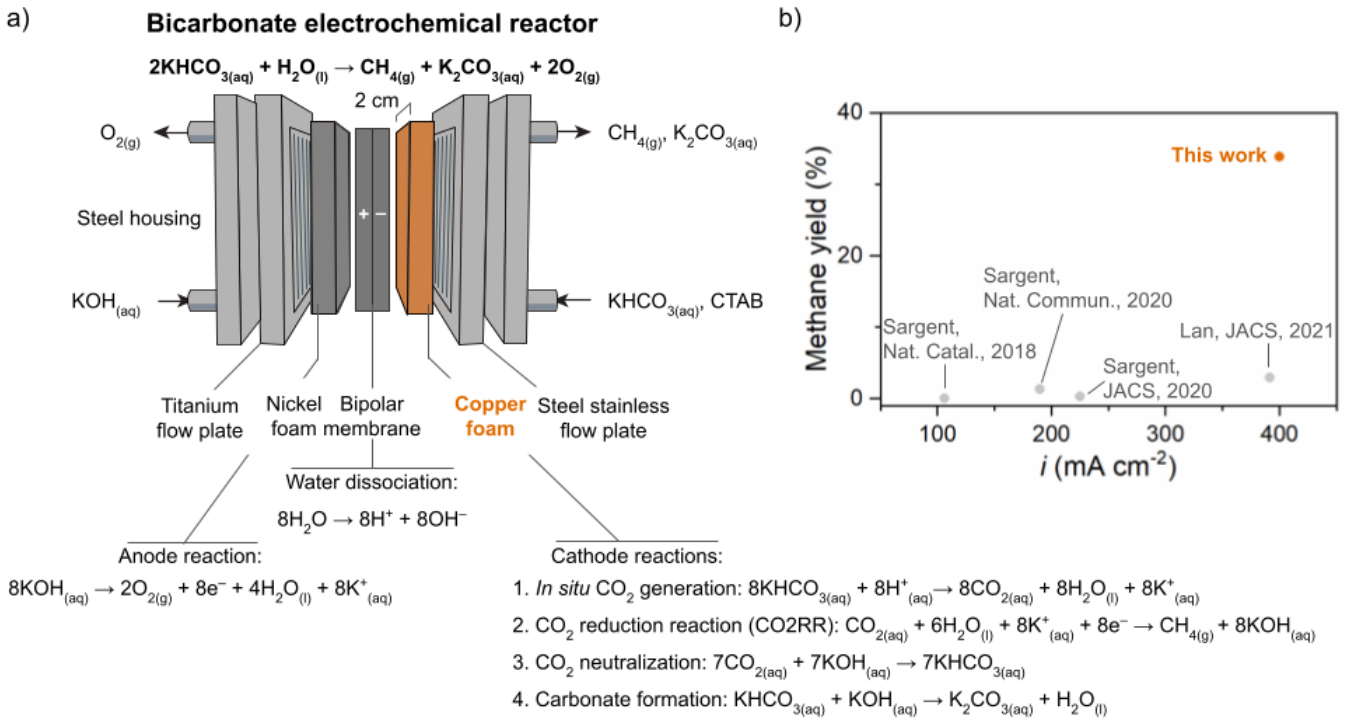

Figure 1: (a) Schematic diagram of the bicarbonate electrochemical reactor used to produce CH_4 from a reactive carbon solution. A bipolar membrane (BPM) separates the nickel foam anode and copper foam cathode. 1 M KOH and 3 M $KHCO_3$ solutions are fed to the anode and cathode compartments, respectively. (b) Methane yields reported in literature as a function of current density (i) for CO_2 electrochemical reactor studies performed at $i_{CH4} > 100$ mA cm^{-2}.[23–26] Methane yield (defined as the molar ratio of methane to unreacted CO_2 in the product stream) was determined using a carbon mole balance where the molar flow rate of unreacted CO_2 was calculated by subtracting the reported inlet molar flow rate of CO_2 from the total moles of carbon atoms in the reduced carbon species (e.g., methane, formate, ethylene, etc.).

The bicarbonate electrochemical reactor used in this study contained a MEA with an active area of 4 cm^2 sandwiched between anodic and cathodic serpentine flow plates.[6] Within the MEA, a bipolar membrane (BPM) consists of an anion exchange layer (AEL) pressed against a cation exchange layer (CEL). A catalyst layer (made of either metal or graphene oxides) at the AEL|CEL interface mediates water dissociation under a reverse-bias to transport OH^- and H^+ to the anode and cathode, respectively.[27] The OH^- is reduced to O_2 and H_2O at the nickel foam anode.[28] The H^+ reacts with HCO_3^- at the CEL|cathode interface to form i-CO_2 (**Eq. 1**).[6] i-CO_2 that is formed by this reaction is electrochemically reduced by a porous copper cathode fabricated by etching copper foam with 3 vol % nitric acid.

Scanning electron microscopy (SEM) show an approximate pore size of 10 μm for the porous copper electrodes (**Fig. S1**).

For bicarbonate electrochemical reactor testing, 3 M $KHCO_3$ solutions containing a cationic surfactant (cetrimonium bromide; CTAB) at concentrations ranging from 0 to 10 mM were delivered to the cathode flow plate. A 1 M KOH solution was delivered to the anode flow plate. Gaseous N_2 was sparged into the catholyte reservoir to sweep the gaseous species (CH_4, CO, CO_2, H_2) from the electrochemical reactor to a gas chromatograph (GC) to determine the faradaic efficiency (FE) and methane yield (see Supporting Information for details). Liquid CO2RR product, formate, was quantified by proton nuclear magnetic resonance (^{1}H NMR) analysis of electrolyte aliquots after 20 min of electrolysis. Control experiments were performed with an analogous electrochemical reactor containing an anion exchange membrane (AEM) (**Fig. S3**). This electrochemical reactor produced formate, but no methane was observed over a range of cathode potentials (–1.75 to 2.3 V vs. Ag/AgCl/KCl saturated) (**Fig. S3a**) and current densities (**Fig. S4**). These results confirm that a supply of H^+ is key to forming methane from reactive carbon solutions.

The cumulative FE for the CO2RR and HER was measured to be 88% on average (range: 74% to 100%) for all electrochemical reactor experiments (**Fig. S5**). The concentration of CTAB in the electrolyte did not have a pronounced effect on the cumulative FE for the CO2RR and HER. We assume that formate accounts for the remaining 12% of FE, but this value is difficult to quantify because formate that accumulates in the MEA would not be detected by the post-electrolysis ^{1}H NMR analyses.

The electrolysis experiments performed without CTAB yielded a maximum partial current density for CO2RR products (i_{CO2RR}) of 11 mA cm^{-2} (**Fig. 3**). Formate was the only CO2RR product formed during the experiment, and the FE_{H2} values were >87% at applied current densities of 100, 200, 300, and 400 mA cm^{-2} (**Fig S6a**)**.** The addition of 3 mM CTAB to the electrolyte increased the i_{CO2RR} from 11 to 162 mA cm^{-2} (at an applied current density of 400 mA cm^{-2}). Importantly, the FE_{CH4}

increased from 0 to 27% with the addition of 3 mM CTAB (**Fig. 3b** and **Fig. S7**). Formate was the dominant CO2RR product observed at current densities <200 mA cm^{-2} (**Fig. S6b**) and cathode potentials > –2 V vs. Ag/AgCl/KCl saturated (**Fig. S4b**). The cell potentials were >6 V for current densities >300 mA cm^{-2}, largely because of the high overpotential associated with water dissociation within the membrane (**Fig. S8**).[29] CTAB is known to suppress HER and enhance formate formation[30,31] but these studies in H-cells did not yield methane. The i_{CH4} of 120 ± 10 mA cm^{-2} that we report here is significantly higher than all other reports which add CTAB to the electrolyte.[23–26,32–34]

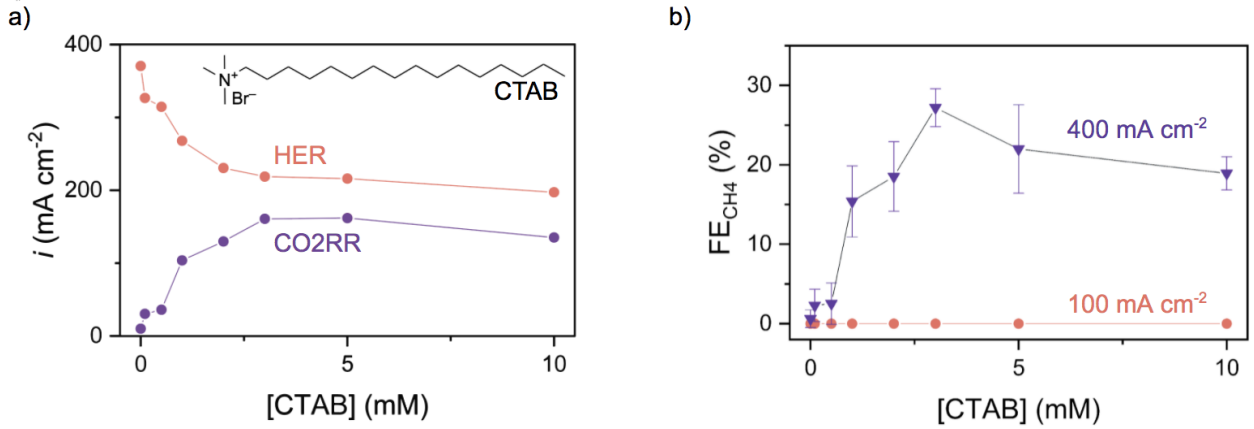

Figure 2: (a) Measured partial current densities for all CO_2 reduction reaction (CO2RR) products (i.e., methane, formate, and carbon monoxide) and the hydrogen evolution reaction (HER) as a function of [CTAB] at an applied current density of 400 mA cm^{-2}. (b) Faradaic efficiencies for methane (FE_{CH4}) measured during electrolysis for bicarbonate solutions doped with CTAB at current densities ranging from 100–400 mA cm^{-2}. Trend lines are provided for each current density as a visual guide.

X-ray diffraction (**Fig. S2)** and *in situ* Raman spectroscopy (**Fig. S9**; see Supporting Information for details)[19] were used to investigate the effect of CTAB on the copper oxidation state. The XRD analysis confirmed the presence of Cu (200), Cu(220), and Cu(111) facets as well as CuO(002) in the etched electrode sample before electrolysis (**Fig. S2**). The CuO peak in the XRD spectra was not observed after the electrolysis experiments performed with CTAB, but it was detected after electrolysis when CTAB was not used (**Fig. S2**). The *in situ* Raman spectroscopy also showed a peak that

corresponds to copper oxide at 530 cm^{-1} for the experiments performed without CTAB at the same current densities (**Fig. S9**).[35] Importantly, this copper oxide peak was not observed for the experiments performed with CTAB. These results imply that CTAB reduces the oxide coverage on the copper electrode during electrolysis.

Previous studies point to the hydrophobic alkyl groups of CTAB in the catalyst microenvironment increasing the ratio of CO_2-to-water near the catalyst surface.[36,37] To confirm this to be the case in our reactor, we ran similar experiments with dodecyltrimethylammonium bromide (DTAB), a quaternary ammonium surfactant with a 12-carbon alkyl chain (the alkyl chains of CTAB contain 16 carbon atoms; **Fig. S10**). The DTAB-doped solution yielded a lower i_{CO2RR} (89 ± 5 mA cm^{-2}) than the CTAB-doped solution (162 ± 10 mA cm^{-2}), yet both surfactants yielded a similar distribution of CO2RR products (**Fig. S10**). Indeed, methane made up 50% of CO2RR products for both CTAB and DTAB at the peak i_{CO2RR} (**Fig S11**). Given that the shorter alkyl chain of DTAB makes the hydrophobic domain smaller than that of CTAB, and there exist different rate limiting steps for methane, formate, and carbon monoxide syntheses, these results are consistent with CTAB increasing the molar ratio of CO_2-to-water at the catalyst surface relative to DTAB.[38]

We developed and applied a 1D finite-element model for the cathode compartment of a bicarbonate electrochemical reactor to investigate the link between pH and methane formation (**Fig. 3**). The model consists of two homogeneous porous domains: the copper catalyst layer, and the cation exchange layer of the bipolar membrane. The governing equations for mass, charge, and fluid transport were solved simultaneously to predict the product distribution during bicarbonate electrolysis. Cathodic transfer coefficients and rate orders for pH and CO_2 from previous studies were used (**Table S1**).[39] These parameters did not account for the use of CTAB or a porous foam electrode,[39] we therefore fit the exchange current densities (i.e., the pre-exponential factors in the CO2RR kinetic expressions) to the experimental data. The intrinsic kinetic factors (e.g., cathodic transfer coefficients, pH and CO_2

dependences) were not modified. The modeled FE_{CH4} increased and the FE_{HCOO-} decreased with increasing current density (**Fig. 3b**). Multi-carbon products have rate limiting steps that are explicitly independent on pH,[16,22] yet none were predicted by the model. The modeled trends in methane and formate formation generally agree with the experiments (**Fig. S6b** and **S7**).

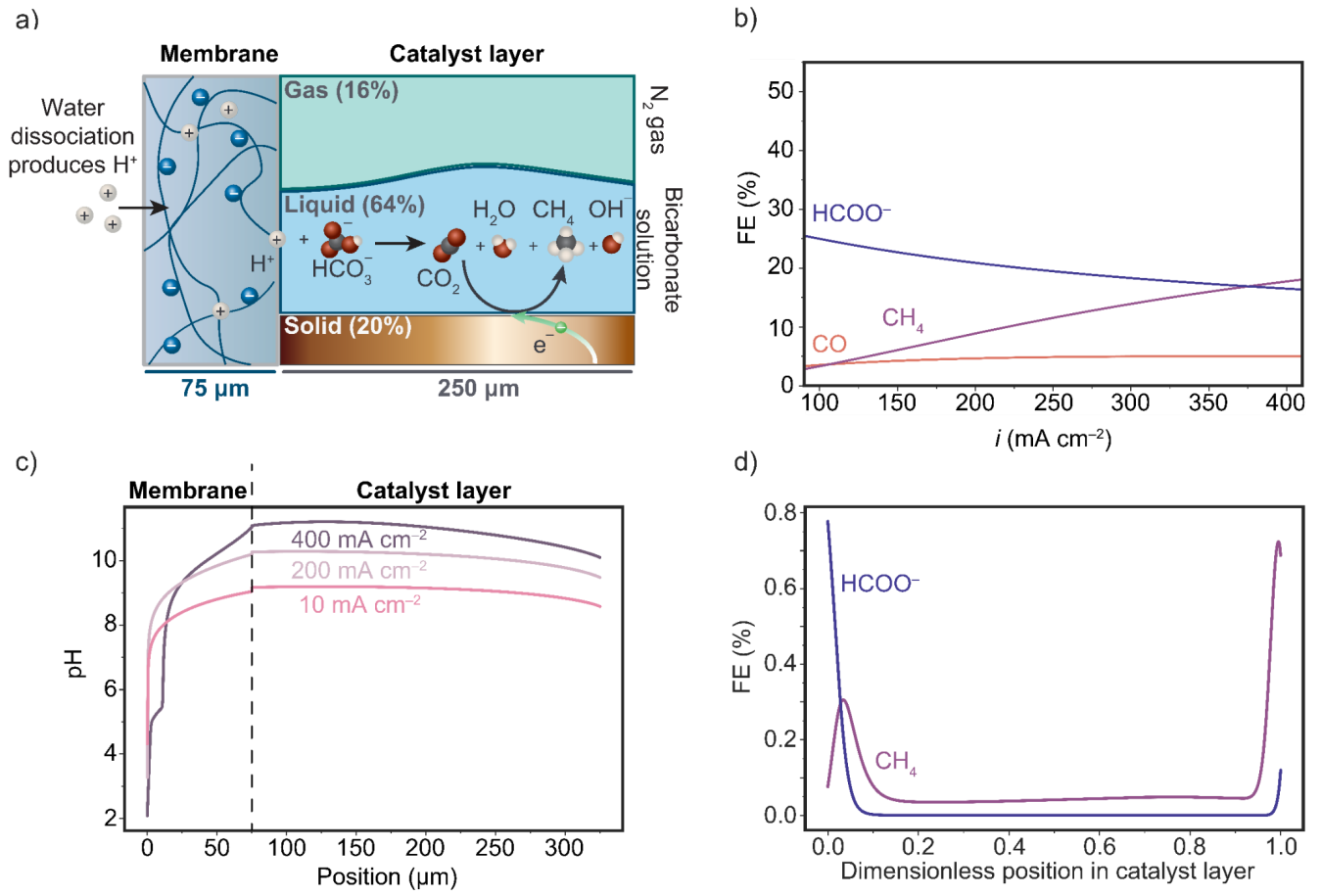

***Figure 3*:** (a) Schematic diagram of the gas, liquid, and solid phases within the membrane (cation exchange layer) and copper catalyst layer domains of the bicarbonate electrochemical reactor. (b) Modeled faradaic efficiency (FE) values for formate, methane, and carbon monoxide as a function of current density. (c) Modeled pH profiles in the membrane and catalyst layer of the bicarbonate electrochemical reactor for current densities ranging from 10 to 400 mA cm^{-2}. (d) Spatial variation in faradaic efficiencies for methane and formate within the modeled catalyst layer domain at a current density of 400 mA cm^{-2}.

The modeled pH in the catalyst layer increased with increasing current density to a maximum value of ~11 at 400 mA cm^{-2} (**Fig. 3c**). This modeled pH is at least 2 pH units lower than previously reported values for electrochemical CO_2 reactors (e.g., 13 at 200 mA cm^{-2})[17] because the H^+ flux from the BPM neutralizes (bi)carbonates and hydroxides at the membrane|catalyst layer interface.[40] This mitigation of cathode alkalinity enables our bicarbonate electrochemical reactor to produce methane at current densities that yield multi-carbon products in other electrochemical CO_2 reactors (**Fig. 3b**).[41]

The H^+ flux from the BPM affects the concentration of CO_2 in the catalyst layer, and, in turn, the spatial distribution of formate and methane formation (**Fig. 3d**). Formate production is second-order in $[CO_2]$,[42] and thus formate is favored at the membrane|catalyst layer interface, where the highest concentrations of CO_2 are found (**Fig. S12**). Methane formation rate has an approximately first-order dependence on $[CO_2]$.[42] This reaction order implies that methane is favored in the bulk of the catalyst layer where there is a lower $[CO_2]$ (**Fig. S12**). Consequently, the maximum modeled FE_{CH4} was observed within the first 5% of the depth of the catalyst layer (**Fig. 3d**), where the $[CO_2]$ and formate formation rates drop off.

Methane formation is also promoted at the catalyst layer|flow plate interface. The bulk pH 8.5 solution and moderate $[CO_2]$ of 8 mM provide favorable conditions for methane formation. These results suggest that thinner cathodes that enable faster mass transport would reduce catalyst loading without sacrificing methane formation rates. The use of an ionomer could improve the methane formation rates by managing the local pH[22] and enhancing the diffusion of CO_2 to the catalyst surface.[43] Collectively, the model results corroborates our experiments and shows how a moderately alkaline pH (<12) at the cathode enables electrochemical methane synthesis at high rates.

We calculated the overall energy required to capture and convert CO_2 into a pure stream of methane using the bicarbonate electrochemical reactor (**Table S2**).[24] For this analysis, we considered the energy required to capture CO_2 using potassium hydroxide to form reactive carbon solutions,[5] to convert

the reactive carbon solution into methane using our electrochemical reactor, and to separate unreacted CO_2 from the methane product stream. This analysis shows that 20,000 kJ is required to produce 1 mole of CH_4. This value is high for the unoptimized bicarbonate-to-CH_4 reactor (electrolysis efficiency = 4%), yet it is still less than the 21,000 kJ required for the pathway involving a more efficient electrochemical reactor fed with gaseous CO_2 (electrolysis efficiency = 16%). The pathway with the bicarbonate electrochemical reactor is more energy efficient because the thermal CO_2 desorption step (>175 kJ mol^{-1} CO_2)[44] is bypassed, and because the methane yield is >5-fold higher.

While even a low-efficiency bicarbonate electrolyzer fares well when the energy required to capture and generate high purity CO_2 is considered, there remain many ways to improve the efficiency of this electrolyzer by increasing the FE_{CH4} and reducing the cell voltage. The FE_{CH4} could be improved by, for example, using a thinner electrode,[41] by positioning an insulating porous material between the membrane and cathode to manage H^+ transport,[28] controlling the CO_2-to-water ratio at the catalyst surface.[45] The cell voltage could be reduced by replacing the BPM with a cationic exchange membrane, or by using alternative reactions at the anode.[46]

We will note that the carbon single-pass conversion (i.e., the moles of CO2RR product formed per mole of carbon fed to the cell) for liquid bicarbonate (0.1%) is much lower than for gaseous CO_2 (1.5%). However, this metric is not as important for a liquid-fed reactor. For electrochemical reactors fed with CO_2 gas, the single-pass conversion is directly correlated to the cost of separating methane from unreacted CO_2 in the product stream.[4] For electrochemical reactors fed with bicarbonate, the single-pass carbon conversion does not directly correlate with the cost of product separation because the insoluble methane product separates passively from the liquid bicarbonate feed.[47] Only unreacted CO_2 in the gaseous product stream of the reactor must be separated for a bicarbonate electrochemical reactor. It is for this reason that the methane yield (which quantifies the unreacted CO_2 that must be separated to

produce pure methane) is a more appropriate measure of downstream separation costs for a bicarbonate-fed reactor.

Electrochemical CO_2 reactors use purified CO_2 gas to achieve high methane formation rates. This use of gaseous CO_2 as a feedstock not only requires energy-intensive steps (i.e., thermal CO_2 desorption) for upstream carbon capture, but also downstream product purification. Here we demonstrate for the first time the electrochemical conversion of bicarbonate-based reactive carbon solutions into methane as a means of bypassing thermal CO_2 desorption. We used a cationic surfactant (CTAB) that adsorbed to the copper catalyst layer during electrolysis to enable methane formation at partial current densities of 120 ± 10 mA cm^{-2} and state-of-the-art methane yields of 34 ± 7%. The 1D continuum model of the cathode compartment showed that the H^+ from the BPM in the bicarbonate electrochemical reactor counteracted hydroxide generation at the cathode surface to promote the formation of methane over multi-carbon products. This study demonstrates the possibility of efficient electrochemical CO_2 capture and methane synthesis using a bicarbonate electrochemical reactor.

Conflict of interest statement

Prof. Berlinguette and Mr. Lees have filed a US patent application related to this work.

Supporting Information

Supplemental information for electrochemical reactor experiments; *In-situ* Raman spectroscopy; materials characterization; continuum model theory and parameters; scanning electron microscopy images; x-ray diffraction data; and additional experimental data and modeling results.

Acknowledgements

The authors thank David J. Dvorak for performing scanning electron microscopy imaging (SEM) and X-ray diffraction (XRD) measurements. The authors thank Dr. Zishuai Zhang for valuable discussions. The authors thank Benjamin A. W. Mowbray and Dr. Roxanna S. DeLima for manuscript

and figure editing. The authors are grateful to the Natural Sciences and Engineering Research Council of Canada (CRDPJ 536621 - 18) and TotalEnergies American Services, Inc. (an affiliate of TotalEnergies SE, France) for financial support. This research was undertaken thanks, in part, to funding from: the Max Planck-UBC-UTokyo Center for Quantum Materials; and the Canada First Research Excellence Fund, Quantum Materials and Future Technologies Program; the Canadian Foundation for Innovation (229288); and the Canadian Institute for Advanced Research (BSE-BERL-162173). SEM imaging was performed in the Centre for High-Throughput Phenogenomics at the University of British Columbia, a facility supported by the Canada Foundation for Innovation, British Columbia Knowledge Development Foundation, and the UBC Faculty of Dentistry. E.W.L acknowledges funding from the Natural Sciences and Engineering Research Council of Canada and Killam doctoral fellowships. A.Z.W and J.C.B acknowledge funding through the US Department of Energy, Office of Energy Efficiency and Renewable Energy under contract number DE-AC02-05CH11231. J.C.B. acknowledges funding, in part, by a fellowship award through the National Defense Science and Engineering Graduate (NDSEG) Fellowship Program sponsored by the Army Research Office (ARO).

References

(1) Natural Gas Information – Analysis - IEA https://www.iea.org/reports/natural-gas-information-overview (accessed 2021 -06 -24).
(2) Stolz, B.; Held, M.; Georges, G.; Boulouchos, K. Techno-Economic Analysis of Renewable Fuels for Ships Carrying Bulk Cargo in Europe. *Nature Energy* **2022**, *7*, 1–10.
(3) Shin, H.; Hansen, K. U.; Jiao, F. Techno-Economic Assessment of Low-Temperature Carbon Dioxide Electrolysis. *Nature Sustainability* **2021**, *4* (10), 911–919.
(4) Alerte, T.; Edwards, J. P.; Gabardo, C. M.; O'Brien, C. P.; Gaona, A.; Wicks, J.; Obradović, A.; Sarkar, A.; Jaffer, S. A.; MacLean, H. L.; Sinton, D.; Sargent, E. H. Downstream of the CO2 Electrolyzer: Assessing the Energy Intensity of Product Separation. *ACS Energy Lett.* **2021**, *6* (12), 4405–4412.
(5) Keith, D. W.; Holmes, G.; St. Angelo, D.; Heidel, K. A Process for Capturing CO2 from the Atmosphere. *Joule* **2018**, *2* (8), 1573–1594.
(6) Li, T.; Lees, E. W.; Goldman, M.; Salvatore, D. A.; Weekes, D. M.; Berlinguette, C. P. Electrolytic Conversion of Bicarbonate into CO in a Flow Cell. *Joule* **2019**, *3* (6), 1487–1497.
(7) Li, Y. C.; Lee, G.; Yuan, T.; Wang, Y.; Nam, D.-H.; Wang, Z.; García de Arquer, F. P.; Lum, Y.; Dinh, C.-T.; Voznyy, O.; Sargent, E. H. CO_2 Electroreduction from Carbonate Electrolyte. *ACS Energy Lett.* **2019**, *4* (6), 1427–1431.
(8) Rubin, E. S.; Davison, J. E.; Herzog, H. J. The Cost of CO2 Capture and Storage. *Int. J. Greenhouse Gas Control* **2015**, *40*, 378–400.

(9) Sanz-Pérez, E. S.; Murdock, C. R.; Didas, S. A.; Jones, C. W. Direct Capture of CO2 from Ambient Air. *Chem. Rev.* **2016**, *116* (19), 11840–11876.
(10) Welch, A. J.; Dunn, E.; DuChene, J. S.; Atwater, H. A. Bicarbonate or Carbonate Processes for Coupling Carbon Dioxide Capture and Electrochemical Conversion. *ACS Energy Letters* **2020**, *5* (3), 940–945.
(11) Lee, G.; Li, Y. C.; Kim, J.-Y.; Peng, T.; Nam, D.-H.; Sedighian Rasouli, A.; Li, F.; Luo, M.; Ip, A. H.; Joo, Y.-C.; Sargent, E. H. Electrochemical Upgrade of CO2 from Amine Capture Solution. *Nature Energy* **2020**, *6* (1), 46–53.
(12) Diaz, L. A.; Gao, N.; Adhikari, B.; Lister, T. E.; Dufek, E. J.; Wilson, A. D. Electrochemical Production of Syngas from CO_2 Captured in Switchable Polarity Solvents. *Green Chemistry* **2018**, *20* (3), 620–626.
(13) Fink, A. G.; Lees, E. W.; Zhang, Z.; Ren, S.; Delima, R. S.; Berlinguette, C. Impact of Alkali Cation Identity on the Conversion of HCO3– to CO in Bicarbonate Electrolyzers. *ChemElectroChem* **2021**, *8* (2094). https://doi.org/10.1002/celc.202100408.
(14) Lees, E. W.; Goldman, M.; Fink, A. G.; Dvorak, D. J.; Salvatore, D. A.; Zhang, Z.; Loo, N. W. X.; Berlinguette, C. P. Electrodes Designed for Converting Bicarbonate into CO. *ACS Energy Lett.* **2020**, *5* (7), 2165–2173.
(15) Nitopi, S.; Bertheussen, E.; Scott, S. B.; Liu, X.; Engstfeld, A. K.; Horch, S.; Seger, B.; Stephens, I. E. L.; Chan, K.; Hahn, C.; Nørskov, J. K.; Jaramillo, T. F.; Chorkendorff, I. Progress and Perspectives of Electrochemical CO_2 Reduction on Copper in Aqueous Electrolyte. *Chem. Rev.* **2019**, *119* (12), 7610–7672.
(16) Gattrell, M.; Gupta, N.; Co, A. A Review of the Aqueous Electrochemical Reduction of CO2 to Hydrocarbons at Copper. *J. Electroanal. Chem.* **2006**, *594* (1), 1–19.
(17) Burdyny, T.; Smith, W. A. CO_2 Reduction on Gas-Diffusion Electrodes and Why Catalytic Performance Must Be Assessed at Commercially-Relevant Conditions. *Energy & Environmental Science* **2019**, *12* (5), 1442–1453.
(18) Yang, K.; Kas, R.; Smith, W. A. In Situ Infrared Spectroscopy Reveals Persistent Alkalinity near Electrode Surfaces during CO_2 Electroreduction. *J. Am. Chem. Soc.* **2019**, *141* (40), 15891–15900.
(19) Zhang, Z.; Melo, L.; Jansonius, R. P.; Habibzadeh, F.; Grant, E. R.; Berlinguette, C. P. pH Matters When Reducing CO2 in an Electrochemical Flow Cell. *ACS Energy Lett.* **2020**, *5* (10), 3101–3107.
(20) Lees, E. W.; Mowbray, B. A. W.; Parlane, F. G.; Berlinguette, C. P. Gas Diffusion Electrodes and Membranes for CO_2 Reduction Electrolyzers. *Nature Reviews Materials* **2021**, *7*, 55–64.
(21) Varela, A. S.; Kroschel, M.; Reier, T.; Strasser, P. Controlling the Selectivity of CO_2 Electroreduction on Copper: The Effect of the Electrolyte Concentration and the Importance of the Local pH. *Catal. Today* **2016**, *260*, 8–13.
(22) Kim, C.; Bui, J. C.; Luo, X.; Cooper, J. K.; Kusoglu, A.; Weber, A. Z.; Bell, A. T. Tailored Catalyst Microenvironments for CO2 Electroreduction to Multicarbon Products on Copper Using Bilayer Ionomer Coatings. *Nature Energy* **2021**, *6*, 1026–1034.
(23) Wang, X.; Xu, A.; Li, F.; Hung, S.-F.; Nam, D.-H.; Gabardo, C. M.; Wang, Z.; Xu, Y.; Ozden, A.; Rasouli, A. S.; Others. Efficient Methane Electrosynthesis Enabled by Tuning Local CO2 Availability. *J. Am. Chem. Soc.* **2020**, *142* (7), 3525–3531.
(24) Xu, Y.; Li, F.; Xu, A.; Edwards, J. P.; Hung, S.-F.; Gabardo, C. M.; O'Brien, C. P.; Liu, S.; Wang, X.; Li, Y.; Wicks, J.; Miao, R. K.; Liu, Y.; Li, J.; Huang, J. E.; Abed, J.; Wang, Y.; Sargent, E. H.; Sinton, D. Low Coordination Number Copper Catalysts for Electrochemical CO2 Methanation in a Membrane Electrode Assembly. *Nat. Commun.* **2021**, *12* (1), 2932.
(25) Wang, Y.-R.; Liu, M.; Gao, G.-K.; Yang, Y.-L.; Yang, R.-X.; Ding, H.-M.; Chen, Y.; Li, S.-L.; Lan, Y.-Q. Implanting Numerous Hydrogen-Bonding Networks in a Cu-Porphyrin-Based Nanosheet to Boost CH4 Selectivity in Neutral-Media CO2 Electroreduction. *Angew. Chem. Int. Ed Engl.* **2021**, *60* (40), 21952–21958.
(26) Jiang, K.; Sandberg, R. B.; Akey, A. J.; Liu, X.; Bell, D. C.; Nørskov, J. K.; Chan, K.; Wang, H. Metal Ion Cycling of Cu Foil for Selective C–C Coupling in Electrochemical CO2 Reduction. *Nature Catalysis* **2018**, *1* (2), 111–119.
(27) Vermaas, D. A.; Wiegman, S.; Nagaki, T.; Smith, W. A. Ion Transport Mechanisms in Bipolar Membranes

for (photo)electrochemical Water Splitting. *Sustainable Energy Fuels* **2018**, *2* (9), 2006–2015.
(28) Salvatore, D. A.; Weekes, D. M.; He, J.; Dettelbach, K. E.; Li, Y. C.; Mallouk, T. E.; Berlinguette, C. P. Electrolysis of Gaseous CO_2 to CO in a Flow Cell with a Bipolar Membrane. *ACS Energy Lett.* **2018**, *3* (1), 149–154.
(29) Blommaert, M. A.; Subramanian, S.; Yang, K.; Smith, W. A.; Vermaas, D. A. High Indirect Energy Consumption in AEM-Based CO2 Electrolyzers Demonstrates the Potential of Bipolar Membranes. *ACS Appl. Mater. Interfaces* **2022**, *14* (1), 557–563.
(30) Banerjee, S.; Han, X.; Thoi, V. S. Modulating the Electrode–Electrolyte Interface with Cationic Surfactants in Carbon Dioxide Reduction. *ACS Catal.* **2019**, *9* (6), 5631–5637.
(31) Tao, Z.; Wu, Z.; Wu, Y.; Wang, H. Activating Copper for Electrocatalytic CO2 Reduction to Formate via Molecular Interactions. *ACS Catal.* **2020**, *10* (16), 9271–9275.
(32) Sedighian Rasouli, A.; Wang, X.; Wicks, J.; Lee, G.; Peng, T.; Li, F.; McCallum, C.; Dinh, C.-T.; Ip, A. H.; Sinton, D.; Others. CO2 Electroreduction to Methane at Production Rates Exceeding 100 mA/cm2. *ACS Sustainable Chemistry & Engineering* **2020**, *8* (39), 14668–14673.
(33) Wang, X.; Ou, P.; Wicks, J.; Xie, Y.; Wang, Y.; Li, J.; Tam, J.; Ren, D.; Howe, J. Y.; Wang, Z.; Ozden, A.; Finfrock, Y. Z.; Xu, Y.; Li, Y.; Rasouli, A. S.; Bertens, K.; Ip, A. H.; Graetzel, M.; Sinton, D.; Sargent, E. H. Gold-in-Copper at Low *CO Coverage Enables Efficient Electromethanation of CO2. *Nat. Commun.* **2021**, *12* (1), 3387.
(34) Zhang, L.; Li, X.-X.; Lang, Z.-L.; Liu, Y.; Liu, J.; Yuan, L.; Lu, W.-Y.; Xia, Y.-S.; Dong, L.-Z.; Yuan, D.-Q.; Lan, Y.-Q. Enhanced Cuprophilic Interactions in Crystalline Catalysts Facilitate the Highly Selective Electroreduction of CO2 to CH4. *J. Am. Chem. Soc.* **2021**, *143* (10), 3808–3816.
(35) Zhao, Y.; Chang, X.; Malkani, A. S.; Yang, X.; Thompson, L.; Jiao, F.; Xu, B. Speciation of Cu Surfaces During the Electrochemical CO Reduction Reaction. *J. Am. Chem. Soc.* **2020**, *142* (21), 9735–9743.
(36) Wang, M.; Wan, L.; Luo, J. Promoting CO2 Electroreduction on CuO Nanowires with a Hydrophobic Nafion Overlayer. *Nanoscale* **2021**, *13* (6), 3588–3593.
(37) Xing, Z.; Hu, X.; Feng, X. Tuning the Microenvironment in Gas-Diffusion Electrodes Enables High-Rate CO2 Electrolysis to Formate. *ACS Energy Lett.* **2021**, *6* (5), 1694–1702.
(38) Ross, M. B.; De Luna, P.; Li, Y.; Dinh, C.-T.; Kim, D.; Yang, P.; Sargent, E. H. Designing Materials for Electrochemical Carbon Dioxide Recycling. *Nature Catalysis* **2019**, *2* (8), 648–658.
(39) Bui, J. C.; Kim, C.; Weber, A. Z.; Bell, A. T. Dynamic Boundary Layer Simulation of Pulsed CO2 Electrolysis on a Copper Catalyst. *ACS Energy Lett.* **2021**, *6* (4), 1181–1188.
(40) Lees, E. W.; Bui, J. C.; Song, D.; Weber, A. Z.; Berlinguette, C. P. Continuum Model to Define the Chemistry and Mass Transfer in a Bicarbonate Electrolyzer. *ACS Energy Lett.* **2022**, *7* (2), 834–842.
(41) Tan, Y. C.; Lee, K. B.; Song, H.; Oh, J. Modulating Local CO2 Concentration as a General Strategy for Enhancing C−C Coupling in CO2 Electroreduction. *Joule* **2020**, *4* (5), 1104–1120.
(42) Wang, L.; Nitopi, S. A.; Bertheussen, E.; Orazov, M.; Morales-Guio, C. G.; Liu, X.; Higgins, D. C.; Chan, K.; Nørskov, J. K.; Hahn, C.; Jaramillo, T. F. Electrochemical Carbon Monoxide Reduction on Polycrystalline Copper: Effects of Potential, Pressure, and pH on Selectivity toward Multicarbon and Oxygenated Products. *ACS Catalysis* **2018**, *8* (8), 7445–7454.
(43) Arquer, F. P. G. de; de Arquer, F. P. G.; Dinh, C.-T.; Ozden, A.; Wicks, J.; McCallum, C.; Kirmani, A. R.; Nam, D.-H.; Gabardo, C.; Seifitokaldani, A.; Wang, X.; Li, Y. C.; Li, F.; Edwards, J.; Richter, L. J.; Thorpe, S. J.; Sinton, D.; Sargent, E. H. CO2 Electrolysis to Multicarbon Products at Activities Greater than 1 A cm−2. *Science* **2020**, *367* (6478), 661–666.
(44) van Straelen, J.; Geuzebroek, F. The Thermodynamic Minimum Regeneration Energy Required for Post-Combustion CO2 Capture. *Energy Procedia* **2011**, *4*, 1500–1507.
(45) Zhu, Q.; Murphy, C. J.; Baker, L. R. Opportunities for Electrocatalytic CO2 Reduction Enabled by Surface Ligands. *J. Am. Chem. Soc.* **2022**, *144* (7), 2829–2840.
(46) Zhang, Z.; Lees, E. W.; Ren, S.; Huang, A.; Berlinguette, C. P. Electrolytic Conversion of Bicarbonate Solutions to CO At> 500 mA Cm-2 and 2.2 V. *ChemRxiv. Prepr.* **2021**, *10.26434/chemrxi13665074.v1 D O I: 10.26434/chemrxiv.13665074.v1*.

(47) Li, M.; Irtem, E.; van Montfort, H. P. I.; Burdyny, T. Sequential vs Integrated CO2 Capture and Electrochemical Conversion: An Energy Comparison. *ChemRxiv* **2021**. https://doi.org/10.26434/chemrxiv-2021-33k4d.